

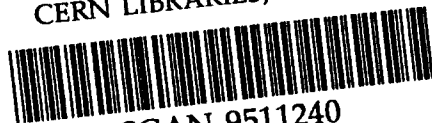
NORDITA preprint

NORDITA - 95/62 N

PARITY VIOLATING ${}^6\text{Li} (0^+1) \rightarrow \alpha + d$ DECAY AND

${}^6\text{Li} (0^+1) \rightarrow \alpha + d + \gamma$ M1 TRANSITION

CERN LIBRARIES, GENEVA



SCAN-9511240

509549

L.V. Grigorenko.¹

Chalmers University of Technology and Göteborg University,
S-41296 Göteborg, Sweden and Nordita.

N.B. Shul'gina.¹

Nordita and NBI, Blegdamsvej 17, DK-2100 Copenhagen Ø, Denmark.

Submitted Phys. Rev. C.

¹Permanent address: Russian Research Center "The Kurchatov
Institute", 123182 Moscow, Russia.

NORDITA · Nordisk Institut for Teoretisk Fysik

Blegdamsvej 17 DK-2100 København Ø Danmark

PARITY VIOLATING ${}^6\text{Li} (0^+) \rightarrow \alpha + d$ DECAY AND ${}^6\text{Li} (0^+) \rightarrow \alpha + d + \gamma$ M1 TRANSITION

L.V. Grigorenko¹,

Chalmers University of Technology and Göteborg University, S-41296 Göteborg, Sweden
and NORDITA

N.B. Shul'gina¹

NORDITA and NBI, Blegdamsvej 17, DK-2100 Copenhagen Ø, Denmark

Abstract

Parity violating ${}^6\text{Li}^* (J^\pi T = 0^+ 1, E = 3.563 \text{ MeV})$ decay to $\alpha + d$ continuum is studied theoretically. Three-body $\alpha + N + N$ wave function is used for ${}^6\text{Li}$ and an optical model for the $\alpha + d$ channel. The parity forbidden width of ${}^6\text{Li} (0^+)$ is found to be within the interval: $\Gamma_{pv} = (0.16 - 0.92) \times 10^{-8} \text{ eV}$, depending on model assumptions about short-range nucleon-nucleon correlations. It is shown that the parity violation effect could be masked by the background M1 decay $\alpha + d + \gamma$ if an experimental energy resolution were not high enough. The background process is connected in a straightforward way with recently measured β -decay of the ${}^6\text{He}$ halo nucleus to $\alpha + d$ continuum and can also be used as a tool for an investigation of the halo structure.

¹ Permanent address: Russian Research Center "The Kurchatov Institute", 123182 Moscow, Russia

1 Introduction

In spite of the fast and successful development of high-energy physics, nuclei have been and remain the important source of information on weak interaction processes. In essence, nuclei can be considered as a laboratory for studying the low energy aspects of fundamental interactions. Being a good "filter" of quantum numbers, nuclei allow us to test the different operators of the weak Hamiltonian both in neutral and charged channels. All the expected effects are small at low energies and can be easily masked by nuclear structure uncertainties. Therefore it is necessary to know nuclear matrix elements of tested operators with high accuracy. From this point of view, the lightest nuclei are the most promising tool to probe weak forces, since few-body models of light nuclei have been intensively developed in the last decade, as reviewed in [1].

Investigations of light nuclei having a cluster structure are most advanced. Calculations of $A=6$ nuclei, which are considered as an α -cluster and two nucleons in various three-body approaches [2, 3, 4, 5, 6, 7] showed that, using "fundamental" pairwise interactions of constituents, one can describe numerous characteristics of the $A=6$ nuclei in a self-consistent way. Thus, in refs. [4, 5, 8, 9, 10, 11] binding energy, geometric and electromagnetic characteristics, form-factor behaviour for electron scattering, β -decay of ${}^6\text{He}$, energy spectra for ${}^6\text{He}$ fragmentation and cross sections of charge-exchange reactions were calculated reliably. Results of these calculations may be considered as a base for further investigations of weak processes in $A=6$ nuclei, since the nuclear matrix elements are defined with controllable accuracy. In our previous work [12] semileptonic weak interaction in ${}^6\text{Li}$ disintegration by (anti)neutrino was considered and the importance of exact nuclear structure calculations was emphasized. In the present work we focus our attention on the strangeness-conserving nonleptonic weak interactions which can manifest themselves in the parity violating (PV) transition ${}^6\text{Li}^* (J^\pi T = 0^+ 1, E = 3.563 \text{ MeV})$ to the $\alpha + d$ channel.

Parity nonconservation in nuclei is commonly analyzed in terms of parity violating nucleon-nucleon potential, based on one-boson exchange. A comprehensive analysis of parity violation in NN interaction is given in the papers of Escplanques, Donoghue and Holstein [13] and also Adelberger and Haxton [14]. Experimental data on parity forbidden ${}^6\text{Li} (0^+)$ decay were obtained for the first time by D.Wilkinson [15]. The ${}^6\text{Li} (0^+)$ state is situated at 2.088 MeV [30] above the $\alpha + d$ threshold and could decay to the $\alpha + d$ channel (negative parity) due to PV nucleon-nucleon interactions. Experiments [15, 16, 17] look for resonance 3.563 MeV γ -rays in the reaction $\alpha+d$, that could be an evidence of parity forbidden formation of the ${}^6\text{Li} (0^+)$ state. The limits on the PV widths were obtained: $\Gamma_{pv} < 0.2 \text{ eV}$, $\Gamma_{pv} < 1.7 \times 10^{-2} \text{ eV}$, $\Gamma_{pv} < 8. \times 10^{-4} \text{ eV}$ respectively. These values are much higher than the theoretical estimations. In the most precise experiment [18] angular distribution of the recoil ions ${}^6\text{Li}^{++}$ from the reaction $\alpha+d$ was measured. According to this distribution the probability of M1 transition was determined and the PV width was derived as $\Gamma_{pv} < 6.5 \times 10^{-7} \text{ eV}$. Only in ref. [19] the decay of ${}^6\text{Li} (0^+)$ was studied directly (separation of excited ${}^6\text{Li} (0^+)$, coincidence of α and d). Unfortunately, the high background lead to less restrictive upper limit for Γ_{pv} of the ${}^6\text{Li} (0^+)$ state

$\Gamma_{pv} < 0.2$ eV. The width of ${}^6\text{Li}(0^+)$, $\Gamma=8.2\pm 0.2$ eV [30], is governed by $M1$ transition to the ${}^6\text{Li}(1^+)$ ground state. ${}^6\text{Li}(0^+)$ can decay to $\alpha+d$ continuum, irradiating an $M1$ γ -quantum. In the case of a parity violating transition we get monoenergetic deuterons (α -particles). Background events give continuous spectrum which can influence the result of measurements under the following conditions. If we deal with a fusion reaction $\alpha + d$ and the energy width of the beam is high, the background reaction may take place on the tail of an energy distribution where the energy of particles is higher than the resonance energy. In the inverse case, if we observe the decay ${}^6\text{Li}(0^+)$ with a detector having a large energy window we may see particles at the tail of the $\alpha + d + M1$ spectrum. Though the spectrum of $M1$ transition behaves as E^3 near the threshold, we compare electromagnetic and weak processes and it is not clear on beforehand what energy resolution is necessary to neglect $M1$ transition to the α - d continuum. The $M1$ transition to α - d continuum is important not only as a background process for parity forbidden decay. In fact, ${}^6\text{Li}(0^+)$ is the isobar-analog of ${}^6\text{He}(0^+)$ halo nucleus, and the $M1$ ${}^6\text{Li}(0^+)$ decay to α - d continuum should have much in common with ${}^6\text{He}(0^+)$ β -decay to α - d continuum. The latter was measured recently [20] and was found to be very sensitive to specific three-body correlations and to asymptotic behaviour of three-body wave functions [21]. So, the experimental investigation of the $M1$ transition to α - d continuum can provide the important and supplementary information on the halo nuclei structure.

2 ${}^6\text{Li}$ Wave Functions

The wave functions (WF) of $A=6$ nuclei are obtained in a semimicroscopic three-body cluster $\alpha+N+N$ model using the method of *hyperspherical harmonics* (HH) [5, 11]. This method is especially suitable for describing so-called "borromean" systems [1], having no bound subsystems. The $A=6$ isotriplet ($T=1, 0^+$) belongs to this type, so the method is adequate to the problem. In the $\alpha + N + N$ representation of $A=6$ nuclei (see for details [1]), the bound state and 3-body continuum wave functions have the product form

$$\Phi_{JM}^T = \exp(i\mathbf{P} \cdot \mathbf{R})\Phi_\alpha(\zeta_\alpha)\Psi_{JM}^T(\mathbf{X}, \mathbf{Y})$$

where \mathbf{P} and \mathbf{R} are total momentum and coordinate of the center of mass (CM) respectively whereas $\Phi_\alpha(\zeta_\alpha)$ is the α -particle intrinsic WF ($J_\alpha = T_\alpha = 0$), while $\Psi_{JM}^T(\mathbf{X}, \mathbf{Y})$ is the "active" part of the three-body WF carrying the total angular momentum J , its projection M and total isospin T . It depends on relative coordinates and nucleon spins (suppressed in our notations) and is the object of the calculation.

It is convenient to introduce translationally invariant normalized sets of Jacobi coordinates \mathbf{X} and \mathbf{Y} , say

$$\begin{aligned} \mathbf{x}_3 &= (A_{12})^{1/2}\mathbf{X}_{12} = (A_{12})^{1/2}(\mathbf{R}_2 - \mathbf{R}_1) \\ \mathbf{y}_3 &= (A_{(12)3})^{1/2}\mathbf{Y}_{(12)3} = (A_{(12)3})^{1/2}[(\mathbf{R}_3 - (A_1\mathbf{R}_1 + A_2\mathbf{R}_2)/(A_1 + A_2))] \\ \mathbf{R} &= (\mathbf{R}_1 + \mathbf{R}_2 + \mathbf{R}_3)/A \end{aligned}$$

where $A_{12} = A_1A_2/(A_1 + A_2)$ is the reduced mass number for the pair (1,2) (with scaling mass m , that of the nucleon); similarly for the CM of (1,2) with respect to the particle 3, i.e. $A_{(12)3} = (A_1 + A_2)A_3/(A_1 + A_2 + A_3)$; $A = (A_1 + A_2 + A_3)$. In our particular case \mathbf{X} is the relative distance between valence nucleons and \mathbf{Y} is the vector from the α -particle to the NN center of mass.

$$\mathbf{x} = \sqrt{\frac{1}{2}}\mathbf{X} = \sqrt{\frac{1}{2}}\mathbf{r}_{12} \quad \mathbf{y} = \sqrt{\frac{4}{3}}\mathbf{Y} = \sqrt{\frac{4}{3}}\mathbf{r}_{(12)3}$$

Alternative sets of Jacobi coordinates are obtained by cyclic permutations of (1,2,3). We introduce hyperspherical coordinates ρ and θ ,

$$\begin{aligned} \rho^2 &= (x^2 + y^2) = \sum_{i=1}^3 A_i r_i^2 & \theta &= \arctan(x/y) \\ x &= \rho \sin(\theta) & y &= \rho \cos(\theta) \end{aligned}$$

Here the hyperradius ρ is a collective rotationally and permutationally invariant variable, while the hyperangle θ has a corresponding three-body hypermoment with quantum number $K = l_x + l_y + 2n$ ($n = 0, 1, 2, \dots$), l_x is relative N-N orbital momentum, l_y is (N-N) orbital momentum relatively to α -particle.

$\Psi_{JM}^T(\mathbf{X}, \mathbf{Y})$ is a standard HH method WF in LS coupling

$$\Psi_{JM}^T(\mathbf{X}, \mathbf{Y}) = \rho^{-5/2} \sum_{K=k_{min}, \gamma}^{k_{max}} \chi_{K,\gamma}(\rho) \mathcal{J}_{K,\gamma}(\Omega_5) \quad (1)$$

$$\gamma = \{l_x, l_y, L, S\}$$

where $k_{min} = l_x(min) + l_y(min)$ - the lowest possible K depending on lowest possible angular momenta; k_{max} the highest K truncating the basis according to computational opportunities. In this expressions we used hyperspherical harmonics (HH) $\mathcal{J}_{K,\gamma}(\Omega_5)$ (where $\Omega_5 = \{\theta, \hat{n}_x, \hat{n}_y\}$) having the explicit form:

$$\mathcal{J}_{K,\gamma}(\Omega_5) = \mathcal{J}_{KLS}^{l_x l_y}(\Omega_5) = \psi_K^{l_x l_y}(\theta) \left[\left[Y_{l_x m_x}(\Omega_x) \cdot Y_{l_y m_y}(\Omega_y) \right]_{LM_L} \cdot \chi_S \right]_{JM} \chi_{TM_T}$$

The hyperangular eigenfunctions are expressed in terms of Jacobi polynomials $P_n^{\alpha,\beta}$ by

$$\psi_K^{l_x l_y}(\theta) = N_K^{l_x l_y} (\sin \theta)^{l_x} (\cos \theta)^{l_y} P_{\frac{K-l_x-l_y}{2}}^{l_x+1/2, l_y+1/2}(\cos 2\theta)$$

The WF Ψ_{JM}^T is solution of the Schroedinger three-body equation

$$(T + \hat{V} - E)\Psi_{JM}^T = 0 \quad , \quad \hat{V} = \hat{V}_{12} + \hat{V}_{13} + \hat{V}_{23}$$

When the hyperangular part of WF is separated out, we obtain a set of coupled equations, equivalent to a single particle with the scale mass m (in our calculations we took it equal

to the nucleon mass) moving in a deformed mean field

$$\left(-\frac{\hbar^2}{2m} \left[\frac{d^2}{d\rho^2} + \frac{\mathcal{L}(\mathcal{L}+1)}{\rho^2} \right] + V_{K\gamma, K\gamma}(\rho) - E\right) \chi_{K\gamma}(\rho) = - \sum_{K'\gamma' \neq K\gamma} V_{K'\gamma', K\gamma}(\rho) \chi_{K'\gamma'}(\rho)$$

$$V_{K'\gamma', K\gamma}(\rho) = (\mathcal{J}_{K\gamma}(\Omega_5) | \hat{V} | \mathcal{J}_{K'\gamma'}(\Omega_5))$$

$$\gamma = \{l_x, l_y, L, S\} \quad : \quad \mathcal{L} = K + 3/2$$

Brackets (...) in matrix element denote integration over Ω_5 .

In our case the potential $V_{\alpha N}$ was chosen as in ref. [22] with components fitted to phase shifts of αN scattering in the 0-25 MeV energy range. The Pauli principle was taken into account by using a purely repulsive s -wave αN potential. As was shown in ref. [3] this way of Pauli principle treatment is a good approximation to projecting out of Pauli forbidden states, obtained in a deep s -wave potential. The NN interaction was chosen as a Gogny-Pires-de Tourreil one [23] and includes repulsion at small distances, ls and tensor forces. The Coulomb $\alpha - p$ interaction was also taken into account. The results of the $\Lambda=6$ nuclear wave function calculations are given, for example, in ref. [1]. We show here only the quantum numbers and the percentage for the main components of the ${}^6\text{Li}(0^+1)$ WF :

$$L=S=0 \quad l_x = l_y = 0 - 82.05\% ,$$

$$L=S=1 \quad l_x = l_y = 1 - 14.37\% .$$

The percentage, obtained in another models : 89.5 and 9.5, [4] 87.07 and 12.93, [6] 87.02 and 12.91 [7] is in a good agreement with our values. We would like to draw reader's attention to the relatively large component with $L=1, S=1$. The reason for that is a large spin-orbit α -N interaction which is responsible for the admixture of ($L=1, S=1$) component to the dominant ($L=0, S=0$) one. As we show later, PV ${}^6\text{Li}(0^+1)$ decay proceeds through this admixture.

3 $\alpha+d$ Continuum

An attempt to account exactly for the two-body continuum in the hyperspherical harmonics method is in progress. In the present work we use an approximate approach to the two-body continuum, which is not an exact solution of the three-body Schrödinger equation, but is simulated as a solution of a two-body equation with a α -d potential, fitted to reproduce observed scattering phases.

To show how important final state interactions in the $\alpha+d$ continuum, three different α -d potentials are used, namely: 1) no potential (plane wave continuum), 2) soft Coulomb (potential of homogeneously charged sphere $R=1.4$ fm.), 3) a deep attractive potential with forbidden states [24]. P-wave phase shifts in the potentials differ negligibly for the energies $E < 3$ MeV. Unfortunately, phase shift analysis is too poor for $\alpha+d$ P-wave to refine the potential [24] very much, so all our conclusions are based on the continuum, calculated with the potential [24].

The $\alpha + d$ channel WF was chosen in the product form $\Psi_{\alpha+d} = \Phi_d(\mathbf{x})F_l(k\mathbf{y})$ where $\Phi_d(\mathbf{x})$ is an internal deuteron WF and $F_l(k\mathbf{y})$ is the $\alpha + d$ scattering WF. (For simplicity we omitted the α -particle WF from this formula, and also the spin and isospin terms).

The deuteron WF Φ_d was chosen in a simple analytical form with the correct behaviour at the origin and at large distances.

$$\Phi_d(x) = N_d [1 - \exp(-x/a)^n] \exp(-bx) \quad (2)$$

The value of $1/k = 4.31$ fm is determined by the deuteron binding energy. The parameter a fits the r.m.s. matter radius of the deuteron - 1.96 fm and the normalization of ϕ_d was fixed at $\sim 95\%$ according to the "real" weight of the s -wave component in the deuteron WF. Functions with different n -values correspond to NN potentials with different behavior at short distances. In this way we somewhat simulate different short-range NN correlations. Here, $n = 1$ is a completely attractive potential with Yukawa-like ($\sim -1/r$) behaviour at the origin. Case $n > 1$ corresponds to potentials with singular soft core ($\sim 1/r$), but different WF asymptotics at $r \rightarrow 0$: $\sim r^2$ ($n=2$) and $\sim r^3$ ($n=3$).

Taking into account the selection rules we have to consider only the final states with quantum numbers $L=0, S=1, l_x = 0, l_y = 0$ for $M1$ transition and $L=1, S=1, l_x = 0, l_y = 1$ for parity violating decay to the $\alpha + d$ channel. It means that we can rewrite the $\alpha + d$ channel WF as

$$\Psi_{\alpha+d} = \sum_{l=0,1} \Phi_d(x)F_l(k\mathbf{y}) \quad (3)$$

$\Phi_d(x)$ is the deuteron S -wave components and $F_{l=0,1}(k\mathbf{y})$ is the $\alpha + d$ scattering WF.

For the $M1$ transition, the continuum 3S_1 WF must be orthogonalized (as it should be for an eigenfunction of the three-body Hamiltonian) to the dominant component of ${}^6\text{Li}$ three-body ground state WF having the same quantum numbers $L=0, S=1, l_x = l_y = 0$. The orthogonalization procedure is the same as in ref.[21].

4 Parity Violating N-N Potential

The admixture of states with opposite parity in nuclei arises due to nonleptonic weak processes. A parity violating N-N potential corresponds to them in the static limit. The most general form of the two-body PV potential, based on selection rules only, was given in [25]. According to selection rules $\Delta T = 1$ for the ${}^6\text{Li} (J^\pi T = 0^+1) \rightarrow \alpha + d$ transition, the main contribution to the PV potential comes from one-pion exchange, while ρ -exchange potential, having the same form, is suppressed by a factor of $(m_\pi/m_\rho)^2$ and was neglected in our calculation. As we have already mentioned, in our model ${}^6\text{Li}$ is represented as a structureless α -core ($S=0, T=0$) plus two valence nucleons. In this case a one-pion PV α -nucleon potential reduces to zero while ρ and ω PV α -nucleon exchanges can contribute in principle, but were neglected for the same reason as in the PV nucleon-nucleon potential.

The parity violating one pion-exchange potential has the form [26] :

$$V_{PV}^{\pi}(\mathbf{r}) = \frac{F_{\pi}}{\sqrt{2}} \frac{f_{\pi nn}}{2M} [\vec{\tau}_1 \times \vec{\tau}_2]_3 (\vec{\sigma}_1 + \vec{\sigma}_2) \cdot \vec{r} \frac{d}{dr} \frac{\exp(-m_{\pi} r)}{4\pi r} \quad (4)$$

$$f_{\pi nn}/4\pi = 14.4 \quad F_{\pi} = 5.2 \times 10^{-7}$$

It corresponds to a parity violating meson-nucleon vertex

$$H_{PV}^{\pi nn} = -\frac{F_{\pi}}{\sqrt{2}} \bar{N} [\vec{\tau} \times \vec{\phi}]_3 N$$

The F_{π} value was estimated in [26] by current algebra and PCAC from hyperon decay amplitudes supposing $SU(3)$ symmetry properties of weak currents. Later it was studied using other model assumptions (see e.g. [27]). In ref. [13] different calculation methods for weak NNM vertex constants were analysed (symmetry approach, current algebra and so on) and allowed regions for the constants F_{π} , F_{ρ} , F_{ω} and their "best" values were given. The "best" value $F_{\pi} = 4.6 \times 10^{-7}$ for the Weinberg-Salam model is in a good agreement with a fit to experimental data $F_{\pi} = 5. \times 10^{-7}$ [14]. The latter value was chosen for our calculation.

5 Parity Violating Widths and M1-transitions

5.1 Numerical results

Using ${}^6\text{Li}(0^+1)$ WFs (1), $\alpha+d$ continuum WFs (3) and one pion-exchange PV potential (4), the parity violating widths of the ${}^6\text{Li}(0^+1)$ state was calculated according to formula (5) given below. Formulas (6) and (7) represent parity violating to background M1 probability ratios for fusion and decay type reactions.

$$\Gamma_{pv} = \frac{(2M_{\alpha d})^{3/2} E_R^{1/2}}{8\pi^2} \sum_{s,d} |M_{pv}|^2 d\Omega_k = \frac{(2M_{\alpha d})^{3/2} E_R^{1/2}}{18\pi} \frac{F_{\pi}^2}{M^2} \frac{f_{\pi nn}^2}{4\pi} J_{pv}^2 \quad (5)$$

$$\left(\frac{W_{pv}}{W_{M1}}\right)_{decay} = \frac{8}{9\pi (\Delta E)^4} \frac{F_{\pi}^2 f_{\pi nn}^2 / 4\pi}{e^2 (K_p - K_n)^2} \frac{J_{pv}^2}{J_{M1}^2} \quad (6)$$

$$\left(\frac{W_{pv}}{W_{M1}}\right)_{fusion} = \frac{2}{27\pi (\Delta E)^4} \frac{F_{\pi}^2 f_{\pi nn}^2 / 4\pi}{e^2 (K_p - K_n)^2} \frac{J_{pv}^2}{J_{M1}^2} \quad (7)$$

$$J_{pv} = \frac{1}{k} \int \Psi_{S=1}(X, Y) \frac{1 + m_{\pi} X}{X^2} e^{-m_{\pi} X} \Phi_d(X) F_{l=1}(kY) dX dY$$

$$J_{M1} = \frac{1}{k} \int \Psi_{S=0}(X, Y) \Phi_d(X) F_{l=1}(kY) dX dY$$

where $\Psi_{S=0,1}$ is the ${}^6\text{Li}(0^+1)$ WF component with $L = S = 0$, $l_x = l_y = 0$ and $L = S = 1$, $l_x = l_y = 1$ respectively. Normalization conditions are :

$$\int |\Psi_S(X, Y)|^2 dX dY = N_S \quad \int |\Psi_d(X)|^2 dX = 0.95 \quad F_l(kY) \sim \sin(kY) + \delta - \frac{l\pi}{2} \quad (8)$$

N_S is the percentage of a component with given S-value in ${}^6\text{Li}(0^+1)$. $E_R = 2.088$ MeV is the resonant energy over the two-body threshold, $M_{\alpha d}$ is the reduced mass of the channel and k is the relative α -d momentum. For the decay case ΔE is the energy resolution of the detector. For the fusion case ΔE is widths of the incident beam (energy distribution is considered to be standard gaussian). Probability of the M1 process was obtained by expansion of the $\alpha + d$ spectrum near threshold (it is given here by the phase volume of photons $\sim E^3$) and integration over the energy ΔE in the decay case, or folding with the energy distribution of the particles in the beam for the fusion reaction.

The results for PV width are summarized in Table 1. The sensitivity to short-range nucleon-nucleon correlations is high. PV width Γ_{pv} decreases from 0.92×10^{-8} eV to 0.16×10^{-8} eV when the nucleon-nucleon potential changes from one having at low distances behavior $\sim -1/r$ (Yukawa-like) to $\sim 1/r$ (like Reid Soft Core). This range is given for *deep* α -d potential [24]. The results for plane wave and soft Coulomb continuum are not included in this range; they are presented to feel the influence of the final state interaction. Table 2 contains the relations of the PV process probability to the probability of the background M1 decay for two types of reactions (decay and fusion) and different energy resolution of the experiment. One can see that resolution $\Delta E \sim 70$ keV is not sufficient to distinguish between the process and the background. This condition is not very restrictive and is satisfied in the experiment [18], where $\Delta E \sim 1$ keV. Our upper value $\Gamma_{pv} = 0.92 \times 10^{-8}$ eV is in an agreement with evaluation [28]: $\Gamma_{pv} = 1.5 \times 10^{-8}$ eV and by several orders of magnitude higher than in ref. [29]: $\Gamma_{pv} = 8. \times 10^{-11}$ eV (for the comparison with our result both widths were recalculated for the value $F_{\pi} = 5 \times 10^{-7}$, adopted in the present work). The reason for the discrepancy is the following. The admixture of the states with $S=1$ in ${}^6\text{Li}(0^+1)$ was unknown for the authors of ref. [29] and they estimated this value as negligible. In three-body models the admixture arises due to spin-orbit α -N interaction, which is strong enough to give around 14% $S=1$, $L=1$ contribution to ${}^6\text{Li}(0^+1)$ WF normalization and to provide our Γ_{pv} estimate. The paper [29] supports to some extent our assumption, that the contribution to PV width from α -N one-boson exchange is negligible relatively to the N-N contribution.

We should stress again that the intensity of PV decay is directly connected with the weight of admixture $L=1$, $S=1$ component in ${}^6\text{Li}(0^+1)$. The weight, used here is confirmed by the results, obtained in another models of $A=6$ nuclei. However, in the next section we will show that the experimental data may indicate a decreasing of this component in ${}^6\text{Li}(0^+1)$.

5.2 M1 ${}^6\text{Li}(0^+1) \rightarrow \alpha + d + \gamma$ transition as a tool for the halo structure investigation

The M1 transition to continuum is not only a background for PV forbidden $\alpha+d$ decay but has a serious theoretical interest itself. Indeed, in the framework of any three-body $\alpha + 2N$ approach there is 20 % disagreement between matrix elements deduced from experimental β -decay data ${}^6\text{He} \rightarrow {}^6\text{Li}(1^+) + e^- + \nu$, measured with an accuracy $\approx 0.1\%$ and the M1 ${}^6\text{Li}(0^+) \rightarrow {}^6\text{Li}(1^+) + \gamma$ transition width, measured with an accuracy $\approx 2\%$.

In the long wave limit M1 transition operator \mathbf{O}_j^λ (j - number of nucleon) can be written in the form:

$$\mathbf{O}_j^\lambda = -\frac{\lambda q e}{4M} \{ (K_n + K_p - 1/2) \sigma_j^\lambda + [L_j^\lambda + (K_p - K_n) \sigma_j^\lambda] \tau_j^0 \} \quad (8)$$

where q is γ -ray momentum, $K_p = 2.79$, $K_n = -1.91$, $e^2 = 1/137$. According to selection rules only the $(K_p - K_n) \sigma_j^\lambda \tau_j^0$ term in (8) contributes to the M1 transition.

If isospin is a good symmetry, only slightly violated by Coulomb interactions, the following relation should be valid:

$$\langle 1 || \sigma || 0 \rangle_{M1} = \langle 1 || \sigma || 0 \rangle_\beta$$

The isospin symmetry violation in the ${}^6\text{Li}$ (0^+) state was studied in [7] and was found to be around 0.1%. The comparison of ME $\langle 1 || \sigma || 0 \rangle$ extracted from ${}^6\text{He}$ β -decay and from M1 transition of ${}^6\text{Li}$ (0^+) (using vacuum values of the axial-vector constant renormalization, G_A , and of the isovector nucleon magnetic moment, $K_n - K_p$) show the inconsistency of the experimental results :

$$\langle 1 || \sigma || 0 \rangle_{M1}^2 = 3.96 \pm 0.08 \quad (9)$$

$$\langle 1 || \sigma || 0 \rangle_\beta^2 = 3.26 \pm 0.004 \quad (10)$$

In terms of $\chi_{LS}(\rho)$ functions, defined by Eq.(1), the matrix element has the form:

$$\langle 1 || \sigma || 0 \rangle^2 = 4 \left[\int (\chi_{01}^f \chi_{00}^i - \chi_{10}^f \chi_{11}^i / \sqrt{3}) d\rho \right]^2 \quad (11)$$

Where χ^f is the ${}^6\text{Li}(1^+0)$ ground state WF; χ^i are the ${}^6\text{He}(0^+1)$ WF for β -decay and the ${}^6\text{Li}(0^+1)$ WF for M1 transition. Quantum numbers l_x and l_y are omitted: they should be the same for "i" and "f" functions.

All theoretical predictions support the value (10). Let us assume that the experimental data are correct. In this case the disagreement could mean

either : 1) the nuclear structure of ${}^6\text{Li}(0^+1)$ essentially differs from that of ${}^6\text{He}(0^+1)$ (for example, the experimental value (9) could easily be obtained from Eq.(11) if the admixture of S=1 component in ${}^6\text{Li}(0^+1)$ were nearly zero);

or : 2) mesonic exchange currents contribute a lot in β -decay and M1 transition in A=6 nuclei, increasing M1 and/or decreasing β -decay probabilities.

To probe the nuclear structure it would be worthwhile to measure the M1 transition to the continuum and compare the results with recently measured ${}^6\text{He}$ β -decay to the continuum. As was shown in ref. [21] the probability of ${}^6\text{He}$ β -delayed deuteron emission is very sensitive to WF's asymptotic behaviour, in other words, to the halo structure. We can expect the same for the M1 transition to the α +d continuum. The spectrum of ${}^6\text{Li}(\gamma,d)\alpha$ can easily be obtained by means of the model developed in [21]. Few points of this spectrum were calculated to evaluate this process as a background for PV decay of ${}^6\text{Li}$ (0^+1) and indirectly presented in the Table 2. For the total branching we present here

the result obtained from the experimental branching of ${}^6\text{He}$ β -decay to the continuum and corrected for the relevant phase volume:

$$Br(M1) = \frac{W({}^6\text{Li}(0^+) - \alpha + d + \gamma)}{W({}^6\text{Li}(0^+) - {}^6\text{Li}g.s. + \gamma)} \sim 8. \times 10^{-5} \quad (12)$$

The following conclusions could be made from measurements of the M1+ α +d spectrum.

1) If the $\langle \sigma \tau^- \rangle$ matrix element, extracted from β -delayed deuteron emission were consistent with the $\langle \sigma \tau^0 \rangle$, extracted from M1 deuteron emission, it would mean that the nuclear structure of ${}^6\text{He}$ and ${}^6\text{Li}$ (0^+1) nuclei is nearly the same and isospin is a good symmetry in A=6 nuclei.

2) The quenching (or enhancement) of M1 deuteron emission probability relatively to that for β -delayed deuteron emission would imply that the current theoretical description of the ${}^6\text{Li}$ (0^+1) state is not adequate and the structure of this state differs essentially from the ${}^6\text{He}$ ground state in contradiction to numerous theoretical calculations [4, 5, 6, 7].

6 Conclusion

We evaluated parity violating widths for ${}^6\text{Li}$ (0^+1) decay to α +d continuum: $\Gamma_{pv} = (0.16 - 0.92) \times 10^{-8}$ eV. All the theoretical results, obtained under different assumptions about short range N-N correlations, are by two order of magnitude lower than available experimental precision: $\Gamma_{pv} < 6.5 \times 10^{-7}$ eV [18].

We studied M1 transition to (from) α +d continuum as a background in the PV experiment on ${}^6\text{Li}$. It is shown that the M1 transition can influence significantly when the experimental energy resolution is within the interval 50-100 KeV and dominates when the energy resolution is worse than 100 KeV.

The M1 transition to the α +d continuum may also be an interesting experimental question, leading to a practically model independent comparison with ${}^6\text{He}$ β -delayed deuteron emission data [20]. The latter have a great theoretical interest and have not got an accurate theoretical explanation yet. So, as it is discussed in Sec. 5.2, the results of M1 transition measurements in the α +d continuum could shed a light on the halo structure and transitions of the A=6 nuclei.

7 Acknowledgments

We are very grateful to P.Herczeg, I.Towner, M.Zhukov and J.Bang for useful discussions. This work was done under the financial support from NORDITA, NBI, the Danish National Research Council and the International Science Foundation (grant N M7C000).

References

- [1] M.V. Zhukov, B.V. Danilin, D.V. Fedorov, J.M. Bang, I.J. Thompson, J.S. Vaagen, Phys. Rep. **231** (1993) 151
- [2] J.M. Bang and C. Gignoux, Nucl. Phys. **A213** (1979) 119
- [3] W.C. Parke, and D.R. Lehman, Phys. Rev. **C29** (1984) 2319; A. Eskandarian, D.R. Lehman and W.C. Parke, Phys. Rev. **C38** (1988) 2431
- [4] V.I. Kukulín, V.M. Krasnopol'sky, V.I. Voronchev and P.B. Sazonov, Nucl. Phys. **A453** (1986) 365; V.I. Kukulín, V.N. Pomerantsev, Kh.D. Razikov, V.T. Voronchev, G.G. Ryzhikh, Nucl. Phys. **A586** (1995) 151
- [5] B.V. Danilin, M.V. Zhukov, A.A. Korshennikov, L.V. Chulkov and V.D. Efros, Sov. Jour. Nucl. Phys. **49** (1989) 351, 359; *ibid* **53** (1991) 71
- [6] A. Csótó, Phys. Rev. **C48** (1993) 165
- [7] K. Arai, Y. Suzuki and K. Varga, Phys. Rev. **C51** (1995) 2488
- [8] M.V. Zhukov *et al.*, Europhys. Lett. **12** (1990) 307; Europhys. Lett. **13** (1990) 703
- [9] M.V. Zhukov, L.V. Chulkov, B.V. Danilin and A.A. Korshennikov, Nucl. Phys. **A533** (1991) 428
- [10] B.V. Danilin and N.B. Shul'gina, Izv. Akad. Nauk SSSR Ser. Fiz. **5** (1991) 908
- [11] B.V. Danilin, M.V. Zhukov, S.N. Ershov, F.A. Gareev, R.S. Kurmanov, J.S. Vaagen and J.M. Bang, Phys. Rev. **C43** (1991) 2835
- [12] N.B. Shul'gina and B.V. Danilin, Nucl. Phys. **A554** (1993) 137
- [13] B. Desplanques, J. Donoghue, B. Holstein, Ann. Phys. (N.Y.) **124** (1980) 449
- [14] E.G. Adelberger and W.C. Haxton, Ann. Rev. Nucl. Part. Sci. **35** (1985) 501
- [15] D.H. Wilkinson, Phys. Rev. **109** (1958) 1603
- [16] J. Barette *et al.*, Nucl. Phys. **A238** (1975) 176
- [17] E. Bellotti *et al.*, Nuovo Cimento **29A** (1975) 106
- [18] R.G.H. Robertson *et al.*, Phys. Rev. **C29,3** (1984) 755
- [19] K.P. Artemov *et al.*, Yad. Fiz. **14** (1972) 1105
- [20] K. Riisager *et al.*, Phys. Lett. **B235** (1990) 30
- [21] M.V. Zhukov, B.V. Danilin, L.V. Grigorenko and N.B. Shul'gina, Phys. Rev. **C47** (1993) 2937
- [22] S. Sack, L.C. Biedenharn and G. Breit, Phys. Rev. **93** (1954) 321
- [23] D.Gogny, P.Pires and R.de Tourreil, Phys. Lett. **B32** (1970) 591
- [24] V.G. Neudachin *et al.*, Yad. Fiz. **17** (1973) 750
- [25] R.J. Blin-Stoyle, Phys. Rev. **118** (1960) 1605 , P. Herczeg, Nucl. Phys. **48** (1963) 263
- [26] B.H.J. McKellar, Phys. Lett. **B26** (1967) 107
- [27] B.H.J. McKellar, Phys. Rev. Lett **20** (1968) 1542 , M. Gari and J.H. Reid, Phys. Lett **B53** (1974) 237
- [28] R.G.H. Robertson, B.A.Brown, Phys. Rev. **C28,1** 1983 443
- [29] V.V. Burov *et al.*, Phys. G: Nucl. Phys. **10** (1984) L21
- [30] F.Ajzenberg-Selove, Nucl. Phys. **A490** (1988) 1

deuteron	attr. Yukawa	Soft core 1	Soft core 2
$\alpha+d$ potential	n=1, a=1.55 fm	n=2, a=1.54 fm	n=3, a=1.56 fm
Plane wave	5.58	1.69	1.04
Soft coulomb	4.04	1.22	0.75
Deep potential	0.92	0.26	0.16

Table 1: The table contains $\Gamma_{pv} \times 10^8$ eV. For deuteron WF parameters (n, a) see eq.(2). $F_\pi = 5. \times 10^{-7}$. "Plane wave" and "Soft Coulomb" α -d continuum are presented here to show a sensitivity of calculations to final state interactions. "Deep potential" and "Soft Coulomb" P-wave phase shifts are indistinguishable up to 7 MeV.

Decay	$\Delta E = 40$ keV	$\Delta E = 70$ keV	$\Delta E = 100$ keV
Soft coulomb	7490.	799.	192.
Deep potential	38.2	4.08	0.98
Repulsion in S-wave	65.1	6.95	1.67
Fusion	$\Delta E = 40$ keV	$\Delta E = 70$ keV	$\Delta E = 100$ keV
Soft coulomb	1692.	209.	50.3
Deep potential	10.1	1.08	0.26
Repulsion in S-wave	17.2	1.83	0.44

Table 2: The table gives relation W_{pv}/W_{M1} as a function of characteristic experimental energy resolution ΔE for different α -d potentials. "Decay" and "Fusion" indicates the type of an experiment.

